A two-dimensional BEM analysis for dynamic stress intensity factor computation of anisotropic piezoelectric solid with a finite crack

Alan T. Tan [1], Sohichi Hirose [2]

1) Department of Civil Engineering, Tokyo Institute of Technology (2-21-1, O-okayama, Meguro-ku, Tokyo 152-8552, E-mail: alantan@qnde.mei.titech.ac.jp)
2) Department of Mechanical and Environmental Informatics, Tokyo Institute of Technology (2-21-1, O-okayama, Meguro-ku, Tokyo 152-8552, E-mail: shirose@cv.titech.ac.jp)

This paper presents a two dimensional boundary element transient analysis in an anisotropic piezoelectric solid with a finite crack. An electric field is produced if the piezoelectric solid changes material dimensions and conversely, it deforms if an electric field is applied. Mechanical motion and electric flow are both considered and are coupled in this problem. Extended or generalized traction (elastic traction and electric displacement) integral equation is applied on one side of the crack. The time domain fundamental solutions obtained by Wang and Zhang for anisotropic piezoelectric solids using Radon transform is the basis for this boundary integral formulation. The formulation and methodology are similar to the 2D analysis for the anisotropic solid [1]. The fundamental solutions are also separated into the static singular and dynamic regular parts [2]. The static singular part of the BEM is further developed to a form that can be easily adopted in writing the computer code with the help of Stroh's formalism. Details for the static singular part (or the elastostatic part) are shown by Wang[3]. Crack opening displacements and relative electric potentials are the BIEs primary unknowns. The presence of two partial derivatives in the static part makes Galerkin method the viable method. Galerkin method is used to regularize the hypersingularity. Thus, double spatial integrals are needed as well as the integral with respect to time and the integral over a unit circle (from the fundamental solution). The static part and the dynamic part integrations are treated differently. For the static part, the integral over the unit circle is determined in explicit form by using residues and the other integrals are analytically performed. For the dynamic part, integrations in time and space are evaluated analytically while the integral over the unit circle is evaluated numerically.

Key words: anisotropic, boundary element method, crack, dynamic, piezoelectric, stress intensity factor

1. Introduction

Piezoelectric materials are materials that produce an electrical field when the material changes dimension as a result of imposed mechanical force. Conversely, applied electrical field will cause the material to change dimensions. Due to this inherent coupling, piezoelectric materials are widely used and are still finding new important applications in both engineering and medical fields such as transducers and other electromechanical devices. Piezoelectric crystals are also very popular as materials for vibration control in structures. However, these crystals or ceramics are brittle and the presence of crack cannot be prevented either during production or during its service life. Thus, the study of cracks in piezoelectric material is gaining popularity. Furthermore, most piezoelectric materials are not isotropic. Most published researches are static analysis Denda and Lua [5], Pan [6] and Rajapakse and Xu [7] to name a few. Denda et al. [8] developed a 2-D time-harmonic BEM for solids of general anisotropy. Shindo et al.[9] formulated an analytical dynamic solution for orthotropic piezoelectric ceramic. To the authors' knowledge, no research has been done on time

domain boundary element analysis for general anisotropic piezoelectric solids.

Similar to all boundary element models, the main difficulty is getting the proper fundamental solutions. Fortunately for this case, Wang and Zhang [2] derived the explicit form of the fundamental solutions for general anisotropic piezoelectric solids.

In this paper, we present a time domain boundary element method (BEM) for fracture analysis of two dimensional anisotropic piezoelectric solid. The objectives of this study are to check the validity of the fundamental solutions and to develop a numerical model for dynamic fracture analysis in general anisotropic piezoelectric solids. Mechanical motion and electric flow are both considered and are coupled in this problem. The generalized traction (elastic traction and electric displacement) integral equation is applied on one side of the crack and only one side of the crack is discretized. The time domain fundamental solutions obtained by Wang and Zhang for anisotropic piezoelectric solids using Radon transform is the basis for this boundary integral formulation. The formulation and methodology are similar to the 2D analysis for the anisotropic solid [1,4]. The fundamental solutions are first decomposed to the static singular part and to the dynamic part [2,4]. Stroh's formalism is then applied to the static singular part, thus, making it easier to be adopted into a computer code. Details for the static singular part (or the elastostatic part) are shown by Wang[3]. Crack opening displacements and relative electric potentials are the BIEs primary unknowns. Due to the presence of two partial derivatives in the static part, Galerkin method is used to regularize the hypersingularity. Thus, double spatial integrals are needed as well as the integral with respect to time and the integral over a unit circle (from the fundamental solution). The static part and the dynamic part integrations are treated differently. For the static part, the integral over the unit circle is determined in explicit form by using residues and the other integrals are analytically performed. For the dynamic part, integrations in time and space are evaluated analytically while the integral over the unit circle is evaluated numerically. Numerical examples are shown and the effects of the piezoelectricity are discussed.

2. Problem statement

Consider a two dimensional homogeneous, infinite and linearly anisotropic piezoelectric solid. The solid is modeled assuming a crack of arbitrary shape. Fig 1. shows the crack model with an applied impact load. The following defines the generalized displacements U_I , generalized stresses $\Sigma_{\alpha I}$, generalized body forces F_I and generalized elasticity tensor $E_{\alpha IJ\beta}$,

$$U_I = \begin{cases} u_I, & I = 1,2,3 \\ \phi, & I = 4 \end{cases} \tag{1}$$

$$\Sigma_{\alpha I} = \begin{cases} \sigma_{\alpha I}, & I = 1,2,3 \\ D_\alpha, & I = 4 \end{cases} \tag{2}$$

$$F_I = \begin{cases} f_I, & I = 1,2,3 \\ -q, & I = 4 \end{cases} \tag{3}$$

$$E_{\alpha IJ\beta} = \begin{cases} c_{\alpha IJ\beta} & I,J = 1,2,3 \\ e_{J\alpha\beta} & I = 4, J = 1,2,3 \\ e_{I\alpha\beta} & J = 4, I = 1,2,3 \\ -\kappa_{\alpha\beta} & I = J = 4 \end{cases} \tag{4}$$

where u_I are the displacements, ϕ is the electric potential , $\sigma_{\alpha I}$ are the stress, D_α are the electric displacement, f_I are the body forces, q is the electric charge density, $c_{\alpha IJ\beta}$ is the elasticity tensor, $e_{I\alpha\beta}$ is the piezoelectric tensor and finally $\kappa_{\alpha\beta}$ is the dielectric permittivity tensor. Using these definitions, the generalized equations of motion and the generalized constitutive equations are written as

$$\Sigma_{\alpha I,\alpha} = -F_I + \rho \delta^*_{IJ} \ddot{U}_J , \tag{5}$$

$$\Sigma_{\alpha I} = E_{\alpha IJ\beta} U_{J,\beta} , \tag{6}$$

where ρ represents the mass density and δ^*_{IJ} is the generalized Kronecker delta and is defined by

$$\delta^*_{IJ} = \begin{cases} \delta_{IJ}, & I,J = 1,2,3 \\ 0, & \text{otherwise} \end{cases} . \tag{7}$$

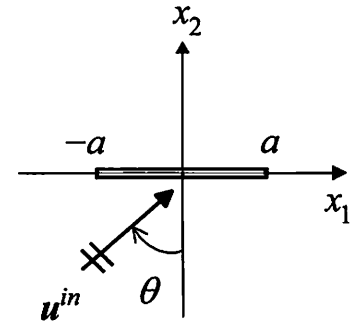

Fig. 1 Crack Model

Throughout this paper, a comma after a quantity denotes partial derivative with respect to the spatial variables while a dot appearing on the top of a quantity denotes partial derivative with respect to time. The summation convention rule over repeated indices is used. Also, lower case roman suffixes take values of 1, 2, and 3 while capital roman suffixes take values of 1, 2, 3, and 4. Greek suffixes have values of 1 and 2 only.

If we substitute Eq.(6) into Eq. (5) and assume zero generalized body forces, the generalized or extended equations of motion are now in terms of the displacement components

$$\left\{\Gamma_{IJ}(\partial_1,\partial_2)-\rho\delta^{*}_{IJ}\partial_t^2\right\}U_J(x,t)=0 \tag{8}$$

where

$$\Gamma_{IJ}(\partial_1,\partial_2)=E_{I\alpha J\beta}\partial_\alpha\partial_\beta \tag{9}$$

is the generalized Cristoffel tensor and ∂_α represents partial derivative.

Zero initial conditions are assumed and on the crack-faces, traction-free boundary conditions are considered. Furthermore, the electric boundary condition on the crack face is assumed to be of the impermeable type. Although studies by Sosa [10] have found out that the boundary in crack faces is actually permeable, the impermeable assumption is used in this paper due to mathematical simplicity. Further studies will be done to check the effect of this assumption.

3. Boundary element equations

Consider a two dimensional elastodynamic problem in a homogeneous anisotropic elastic solid with a finite crack as shown in Fig 1. Using traction free conditions and impermeable electric boundary condition on the crack face, the generalized representation integral for the generalized crack displacement components can be written as:

$$\begin{aligned}U_K(y,t)&=U_K^{in}(y,t)\\&\quad-\int_S H_{IK}\left[(x-y),e(x);t\right]*\Delta U_K(x,t)dx\end{aligned} \tag{10}$$

where x and y are the source and observation point respectively, S is the crack surface and H_{IK} is the generalized traction fundamental solution. * stands for the Riemann convolution. Since the BEM equation leads to a degenerate formulation, the traction boundary integral equation will be used and can be written as:

$$T_J^{in}(y,t)=\int_S W_{IJ}\left[x-y;t\right]*\Delta U_I(x,t)dx \qquad y\in S \tag{11}$$

where T_J^{in} denotes generalized traction component of the incident wave, ΔU_I are the crack opening displacements (CODs) and the relative electric potential difference or the generalized CODs (GCODs), W_{IJ} is the derivative of the stress fundamental solution. The fundamental solution derived by Wang and Zhang [2] is used to obtain W_{IJ} by applying the traction operators twice.

4. Fundamental solutions

The generalized fundamental solution is defined as the solution of the following equations

$$\left\{\Gamma_{PI}(\partial_1,\partial_2)-\rho\delta^{*}_{PI}\partial_t^2\right\}G_{IJ}(x;t)=-\delta^{*}_{PJ}\delta(x)\delta(t) \tag{12}$$

where $G_{IJ}(x;t)=0$ for $t<0$ and $\Gamma_{PI}(\partial_1,\partial_2)=E_{P\beta I\lambda}\partial_\beta\partial_\lambda$.

$G_{km}(x,t)$ is the displacement field in the x_k-direction due to impulsive mechanical point load at $x=0$ in the x_m-direction.

$G_{4m}(x,t)$ is the electric potential field due to an implusive mechanical point load at $x=0$ in x_m-direction. $G_{k4}(x,t)$ is the displacement field in the x_k-direction due to impulsive electrical load at $x=0$. $G_{44}(x,t)$ is the electric potential field due to impulsive electrical point load at $x=0$.

Wang and Zhang [2] using Radon transform derived explicit expressions of the fundamental solutions. Due to the inverse Radon transform the fundamental solution includes an integrand over a unit circle. The integral expressions are given by

$$\begin{aligned}G_{PK}(x,t)&=\frac{H(t)}{4\pi^2}\int_{|n|=1}\sum_{l=1}^{L}\frac{\bar{P}^l_{PK}}{\rho c_l}\frac{dn}{c_l t+n\cdot x}\\&\quad+\frac{1}{2\pi\sqrt{\Lambda}}\log(R)\,\delta_{4P}\delta_{4K}\delta(t)\end{aligned} \tag{13}$$

where

$$\bar{P}^l_{PK}=\begin{cases}P^l_{PK} & P,K=1,2,3,\\ -\dfrac{\Gamma_{i4}P^l_{Pi}}{\Gamma_{44}}, & P=1,2,3,K=4\\ \dfrac{\Gamma_{4i}P^l_{ij}\Gamma_{j4}}{\Gamma_{44}}, & P=K=4\end{cases} \tag{14}$$

and $P^l_{ij}=E_{il}E_{jl}$ are projection operators, E_{ij} and ρc_l^2 are the eigenvectors and eigenvalues of the matrix

$$L_{jk}=\Gamma_{jk}-\frac{\Gamma_{j4}\Gamma_{4k}}{\Gamma_{44}} \tag{15}$$

where $\Gamma_{Pl}(n_1,n_2)=E_{P\beta l\lambda}n_\beta n_\lambda$.

The fundamental solution can be reformulated into two parts, namely static and regular part by applying integration by parts. The singular part corresponds to the elastostatic fundamental solution which has a closed form solution. The higher order fundamental solution can also be separated into its singular static and regular dynamic parts. W_{IJ} is first expressed in time convolution form where $f(t)$ is an arbitrary function.

$$W_{IJ}(x-y;t)*f(t)=W^S_{IJ}(x-y)f(t)+W^R_{IJ}(x-y;t)*\ddot{f}(t) \tag{16}$$

where W^S_{IJ} is the static hypersingular term and W^R_{IJ} is the dynamic regular term. The fundamental solution in separated form is given by

$$\begin{aligned}W^S_{IJ}(x)&=-\frac{1}{4\pi^2}\int_{|n|=1}\sum_{l=1}^{L}\frac{\bar{R}^l_{IJ}}{\rho c_l^2}\frac{1}{(n\cdot x)^2}dn\\W^R_{IJ}(x)&=-\frac{H(t)}{4\pi^2}\int_{|n|=1}\sum_{l=1}^{L}\frac{\bar{R}^l_{IJ}}{\rho c_l^3}\frac{dn}{c_l t+n\cdot x}\end{aligned} \tag{17}$$

where $\bar{R}^l_{IJ}=E_{I\gamma P\delta}e_\gamma(x)n_\delta E_{J\alpha K\beta}e_\alpha(y)n_\beta\bar{P}^l_{PK}(n)$ and e_α is the unit normal vector. The singular part can be further reduced to a closed form expression. The static singular part of the displacement fundamental solution is transformed into an explicit expression by using the residue theorem.

$$G^S_{PK}(x,y)=\frac{1}{\pi}\mathrm{Im}\sum_{l=1}^{L}\left[\frac{A_{PK}(\eta_l)}{\partial_\eta D(\eta_l)}\log(z_l)\right]+C_{PK} \tag{18}$$

where $z_l=x_1-y_1+\eta_l(x_2-y_2)$, $D(\eta_l)=0$ with $\mathrm{Im}(\eta_l)>0$, and L = 4 if all four η_l are distinct. The other terms are given by

$$C_{PK} = -\frac{1}{4\pi^2}\int_{|n|=1}\Gamma_{PK}^{-1}(\boldsymbol{n})\log|n_1|\,d\boldsymbol{n} \tag{19}$$

and $A_{PK}(\eta) = \mathbf{adj}\left[\Gamma_{PK}(1,\eta)\right]$, $D(\eta) = \det\left[\Gamma_{PK}(1,\eta)\right]$, where both are polynomial functions of order six and eight, respectively. If $\Gamma_{PK}^{-1}(1,\eta)$ is well defined, $D(\eta)$ cannot be zero for real η.

The higher order static part can also be reduced to closed form expressions by application of Stroh's formalism [1]. The static part of higher order fundamental solution can be written as

$$W_{IJ}^{S}(\boldsymbol{x}-\boldsymbol{y}) = E_{I\gamma P\delta}e_{\gamma}(\boldsymbol{x})\frac{\partial}{\partial x_{\delta}}E_{J\alpha K\beta}e_{\alpha}(\boldsymbol{y})\frac{\partial}{\partial y_{\beta}}G_{PK}^{S}(\boldsymbol{x}-\boldsymbol{y}) \tag{20}$$

Applying Stroh formalism twice, the static part is given as

$$W_{IJ}^{S}(\boldsymbol{x}-\boldsymbol{y}) = \frac{1}{\pi}\frac{\partial}{\partial s_x}\frac{\partial}{\partial s_y}\mathrm{Im}\sum_{l=1}^{4}\tilde{C}_{IJ}^{l}\log(\boldsymbol{d}_l\cdot(\boldsymbol{x}-\boldsymbol{y})) \tag{21}$$

where

$$\tilde{C}_{IJ}^{l} = \frac{(M_{IP}+L_{IP}\eta_l)A_{PK}(\eta_l)(M_{JK}+L_{JK}\eta_l)}{\partial D(\eta_l)},\quad \boldsymbol{d}_l = (1,\eta_l) \tag{22}$$

and $\Gamma_{ij}(1,\eta) = L_{ij}\eta^2 + (M_{ij}+M_{ij}^{T})\eta + N_{ij}$ where

$$N_{IK} = E_{I1K1},\quad M_{IK} = E_{I1K2},\quad L_{IK} = E_{I2K2}. \tag{23}$$

5. Numerical implementation

In solving the boundary integral equation (11), Galerkin procedure is adopted to reduce the hypersingularity in the static part. Eq. (11) is recasted into a weighted integral sense by multiplying the weighing function, and then integrating over the observation point (field point).

$$\begin{aligned}\int_S \phi_u^m(\boldsymbol{y})T_I^{in}(\boldsymbol{y},t)dS_y = {} & \int_S \phi_u^m(\boldsymbol{y})dS_y\int_S \frac{1}{\pi}\frac{\partial}{\partial s_x}\frac{\partial}{\partial s_y}\times \\ & \mathrm{Im}\sum_{l=1}^{L}\tilde{C}_{IJ}^{l}\log(\boldsymbol{d}_l\cdot(\boldsymbol{x}-\boldsymbol{y}))\Delta U_J(\boldsymbol{x},t)dS_x \\ & + \int_S \phi_u^m(\boldsymbol{y})dS_y\int_S W_{IJ}^{R}(\boldsymbol{x}-\boldsymbol{y};t)*\Delta\ddot{U}_J(\boldsymbol{x},t)dS_x\end{aligned} \tag{24}$$

The partial derivatives are then moved to the weight function and the GCODs using integration by parts twice and with the assumption that the GCODs are zero in the crack tip, which results to

$$\begin{aligned}\int_S \phi_u^m(\boldsymbol{y})T_I^{in}(\boldsymbol{y},t)dS_y = {} & \frac{1}{\pi}\int\frac{\partial\phi_u^m(\boldsymbol{y})}{\partial S_y}dS_y\int_S\frac{\partial\Delta U_J(\boldsymbol{x},t)}{\partial S_x}\times \\ & \mathrm{Im}\sum_{l=1}^{L}\left\{\tilde{C}_{IJ}^{l}(\eta_l)\log(\boldsymbol{d}_l\cdot(\boldsymbol{x}-\boldsymbol{y}))\right\}dS_x \\ & + \int_S \phi_u^m(\boldsymbol{y})dS_y\int_S W_{IJ}^{R}(\boldsymbol{x}-\boldsymbol{y};t)*\Delta\ddot{U}_J(\boldsymbol{x},t)dS_x\end{aligned} \tag{25}$$

The time stepping method is a process used to approximate the values at a finite number of times intervals. Thus, the boundary integral equation is then approximated by linear algebraic system of equations which can be solved using numerical method. The proper selection of the shape functions could make the problem easier to deal with. Similarly, the boundary of the crack is discretized in a finite number of points and a spatial shape function is chosen. The variables or fields in the boundary are approximated as

$$\Delta U_J(\boldsymbol{x},t) = \sum_{q=1}^{Q}\sum_{n=1}^{N}\phi_u^n(\boldsymbol{x})\varphi_u^q(t)\left[\Delta U_J\right]^{nq} \tag{26}$$

where $\phi_u^n(x)$ are the spatial shape function and $\varphi_u^q(t)$ the temporal shape function. $\phi_u^n(x)$ are linear shape functions for this problem while the temporal shape function is chosen as:

$$\varphi_u^q(t) = \frac{1}{\Delta t}\begin{bmatrix}(t-(q-1)\Delta t)H(t-(q-1)\Delta t)\\ -2(t-q\Delta t)H(t-q\Delta t)\\ +(t-(q+1)\Delta t)H(t-(q+1)\Delta t)\end{bmatrix} \tag{27}$$

The second derivative of the temporal shape function is

$$\ddot{\varphi}^q(t) = \frac{1}{\Delta t}\begin{bmatrix}\delta(t-(q-1)\Delta t)-2\delta(t-q\Delta t)\\ +\delta(t-(q+1)\Delta t)\end{bmatrix} \tag{28}$$

Substitution of Eqns (26)-(28) into Eq. (25) leads to a system of linear algebraic equations as follows

$$\sum_{n=1}^{N}D^{mn}T_J^{in,nQ} = \sum_{n=1}^{N}W_{IJ}^{S;mn}\Delta U_I^{nQ} + \sum_{q=1}^{Q}\sum_{n=1}^{N}W_{IJ}^{R;m,n,Q-q+1}\Delta U_I^{nq} \tag{29}$$

where

$$D^{mn} = \int\phi_u^m(\boldsymbol{y})\phi_t^n(\boldsymbol{y})dS_y \tag{30}$$

$$\begin{aligned}W_{ij}^{S;m,n} = {} & \frac{1}{\pi}\int\frac{\partial\phi_u^m(\boldsymbol{y})}{\partial S_y}dS_y\int_S\frac{\partial\phi_u^n(\boldsymbol{x})}{\partial S_x}\times \\ & \mathrm{Im}\sum_{l=1}^{L}\left\{\tilde{C}_{IJ}^{l}(\eta_l)\log(\boldsymbol{d}_l\cdot(\boldsymbol{x}-\boldsymbol{y}))\right\}dS_x\end{aligned} \tag{31}$$

$$W_{ij}^{R;m,n,q} = \int_S\phi_u^m(\boldsymbol{y})dS_y\int_S W_{IJ}^{R}(\boldsymbol{x}-\boldsymbol{y},t)*\ddot{\varphi}_u^q(t)\times\phi_u^n(\boldsymbol{x})dS_x \tag{32}$$

The time convolution of Eq. (32) can be evaluated analytically by using Eq. (28) and is given as

$$\begin{aligned}W_{IJ}^{R}(\boldsymbol{x}-\boldsymbol{y},t)*\ddot{\varphi}_u^q(t) = {} & \int_0^{\varrho}W_{IJ}^{R}(\boldsymbol{x}-\boldsymbol{y},\tau)\ddot{\varphi}_t^q(t^{Q}-\tau)d\tau \\ = {} & \frac{1}{\Delta t}\begin{Bmatrix}W_{IJ}^{R}\left[\boldsymbol{x}-\boldsymbol{y},(Q-(q-1))\Delta t\right]\\ -2W_{IJ}^{R}\left[\boldsymbol{x}-\boldsymbol{y},(Q-q)\Delta t\right]\\ +W_{IJ}^{R}\left[\boldsymbol{x}-\boldsymbol{y},(Q-(q+1))\Delta t\right]\end{Bmatrix}\end{aligned} \tag{33}$$

Since simple linear spatial shape functions are chosen, the integrands are evaluated analytically in time and space. Only the regular part with integral over a unit circle needs to be computed numerically.

6. Dynamic stress intensity factor

Stress intensity factors are used to define the magnitude of the singular stress and displacement. The dynamic stress intensity factors for anisotropic solids can be computed directly and are related to the CODs [1] by:

$$\begin{Bmatrix}K_I\\ K_{II}\end{Bmatrix} = \frac{\sqrt{\pi}}{2\sqrt{2r}D}\begin{bmatrix}\mathrm{Re}\left\{\frac{i}{s_1-s_2}(q_2-q_1)\right\} & \mathrm{Re}\left\{\frac{-i}{s_1-s_2}(p_2-p_1)\right\}\\ \mathrm{Re}\left\{\frac{-i}{s_1-s_2}(s_1q_2-s_2q_1)\right\} & \mathrm{Re}\left\{\frac{i}{s_1-s_2}(s_1p_2-s_2p_1)\right\}\end{bmatrix}\begin{Bmatrix}u\\ v\end{Bmatrix} \tag{34}$$

where D is the determinant of the coefficient matrix, u and v are the displacements parallel and normal to the crack near the crack-tip, r is the distance from the crack tip, and s_J, q_J, p_J are determined from the material compliance matrix.

6. Numerical results

Consider a crack of finite length 2a in an infinite linearly elastic solid subjected to an incident transient dilatational waves directed normal to the crack such that

$$u_2^{in} = -\frac{p_o}{c_{22}}\left(x_2 + c_1 t\right) H\left(x_2 + c_1 t\right)$$
$$\phi^{in} = -\frac{e_{22} p_0}{c_{22}\kappa_{22}}\left(x_2 + c_1 t\right) H\left(x_2 + c_1 t\right) \tag{35}$$

where $c_1 = \sqrt{\bar{c}_{22}/\rho}$ is the compression wave velocity, $\bar{c}_{22} = c_{22} + e_{22}^2/\kappa_{22}$ is the piezoelectrically stiffened elastic constant, p_0 is a constant with dimension stress, and H(t) is the Heaviside step function. Sample materials are taken as PZT-6B and $BaTiO_3$ ceramics with engineering constants listed in Table 1.

Table 1. Material properties of piezoelectric ceramics.

		PZT-6B	BaTiO3
Elastic stiffness (GPa)	c_{11}	168	150
	c_{22}	163	146
	c_{66}	27.1	23
	c_{12}	60	84
Piezoelectric coefficients (C/m^2)	e_{21}	-0.9	-4.35
	e_{22}	7.1	17.5
	e_{16}	4.6	11.4
Dielectric constants ($x10^{-10}$ C/Vm)	κ_{11}	36	34
	κ_{22}	98.7	112

To check the new formulation's accuracy, the piezoelectric coefficients are first assumed to be zero, thus decoupling the effects of mechanical and electrical part. Fig. 2 shows the time variations of $\Delta u_2/u_0$ for the PZT-6B. u_0 is the displacement amplitude of the incident wave. The crack is subdivided into 40 elements of equal size. $c_1\Delta t/a = 0.05$ is taken as the time step. Plane strain is assumed. The present work is compared to the previous general anisotropic model (see Tan et al. [1]). The solid lines with the dot indicate the results obtained from Tan et al. anisotropic model while the unshaded circles are those of the present time-domain BEM with the piezoelectric coefficients set at zero. Both methods show the same values of crack opening displacements.

To examine the effects of the coupling of electrical and mechanical parts, the dynamic stress intensity factor is determined. Figs. 3 and 4 show the result for PZT-6B and $BaTiO_3$, respectively. The stress intensity factors are normalized with the division by $\rho_0\sqrt{\pi a}$. Results are then compared to the results of Shindo et al. [8].

The analytical method of Shindo et.al and the present work shows the normal dynamic SIF curve. The line curves are for the analytical model while the triangular plots are for the present work. The dynamic stress intensity factor has a steep curve before reaching the peak and then decreases in magnitude until it reaches the steady state static solution. On closer examination, difference in values near the peak can be seen between the two models. The analytical solution has a higher value for the dynamic overshoot. It should be noted that the analytical solution considered the permeable electric boundary condition. This could account for the difference in values. For the PZT-6B, both models have the same time where the peak occurs (at about 2.25). While for the $BaTiO_3$, the peak occurs at 2.5 for the analytical one and 2.25 for the present work.

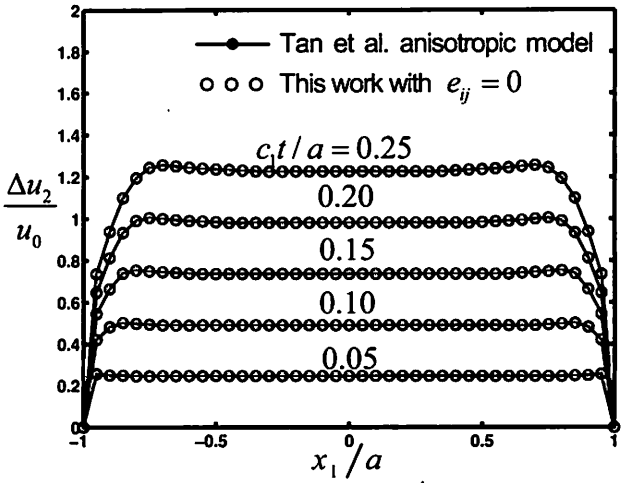

Fig 2. Time variations of $\Delta u_2/u_0$ for a crack and a normal incidence of dilatational wave in PZT-6B

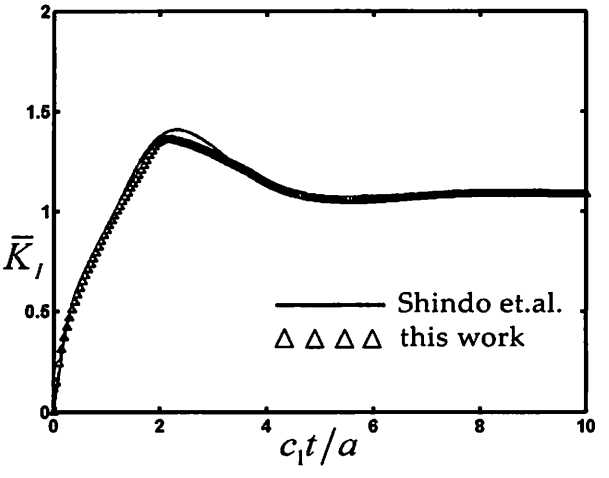

Fig. 3. Normalized dynamic stress intensity factor for PZT-6B

It should also be noted that the present time-domain BEM uses the same explicit time-stepping scheme to that of our previous work. It is considered conditionally stable. The time step should be chosen properly so that the BEM be stable and would have quality results. From our numerical experiences, the

time step should be just enough for the smallest wave velocity to traverse one element. All in all, the results of the present work show good agreement with the analytical ones.

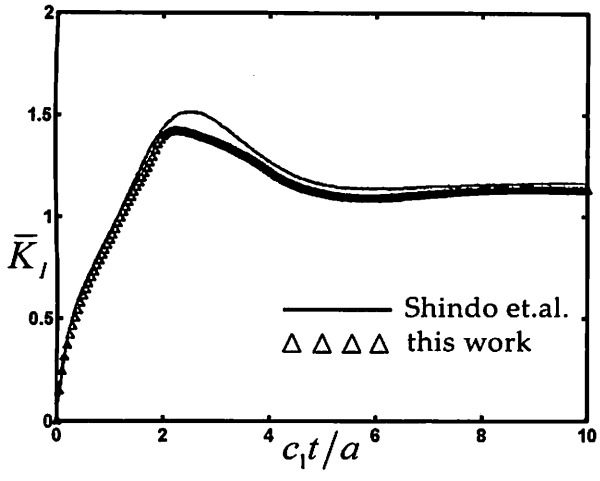

Fig. 4 Normalized dynamic stress intensity factor for $BaTiO_3$

7. Summary

A 2D time-domain traction BEM for piezoelectric solids of general anisotropy with cracks is presented in this paper. The methodology is similar to our previous work [1] except for the coupling between the mechanical motion and electrical flow. The method uses the time domain fundamental solutions for anisotropic piezoelectric solids derived by Wang and Zhang [2]. This method uses the collocation method for the time discretization and the Galerkin method for space. The use of linear temporal and spatial shape functions makes analytical integration possible. Only the integral over the unit circle needs to be done numerically. The accuracy of the present work is verified by showing numerical examples.

For extension of the present work, elliptical cavities would be considered and the development of the displacement time domain BEM is in progress. The displacement time domain BEM can be used for the finite domain problem. The traction time domain BEM can also be extended to solve the finite domain problem. The next step is to check the effect of the permeability of the electrical boundary condition by coupling with the governing equations for the vacuum. The study of the effect of the change in the electrical boundary condition by changing the thickness of the elliptical cavity is of interest. For very thin elliptical cavity, we should be able to approximate the effect of the electrical boundary conditions on the crack problem.

References

(1) Tan, A., Hirose, S., Zhang, Ch. and Wang, C.-Y.: A time-domain BEM for transient wave scattering analysis by a crack in anisotropic solids. *Eng. Anal. with Bound. Elem.*, in press, 2005.

(2) Wang, C.-Y. and Zhang, Ch., 2D and 3D dynamic Green's functions and time-domain BIE formulations for Piezoelectric Solids. *Proceeding in computational mechanics WCCM VI in conjunction with APCOM'04, 2004 Tsinghua University Press & Springer-Verlag*, Beijing China, Sept. 5-10, 2004.

(3) Wang, C.-Y. Green's functions and general formalism for 2D Piezoelectricity. *Appl. Math. Lett. Vol. 9, No. 4*, pp.1-7, 1996.

(4) Wang C.Y., Achenbach, J.D. and Hirose S., Two dimensional time domain BEM for scattering of elastic waves in solids of general anisotropy, *International Journal of Solids and Structures*, Vol. 33, no.26, pp. 3843-3864, 1996.

(5) Denda, M. and Lua, J. Development of the boundary element method for 2D piezoelectricity. *Composites: Part B 30* 699-707, 1999.

(6) Pan, Ernian, A BEM analysis of fracture mechanics in 2D anisotropic piezoelectric solids, *Engineering Analysis with Boundary Elements 23* 67–76, 1999.

(7) Rajapakse, R.K.N.D., Xu, X.-L., Boundary element modeling of cracks in piezoelectric solids. *Engineering Analysis with Boundary Elements 25* pp. 771-781, 2001.

(8) Denda, M., Wang, C.Y. and Yong, Y.K., 2-D time-harmonic BEM for solids of general anisotropy with application to eigenvalue problems. *Journal of Sound and Vibration 261* pp. 247-276, 2003.

(9) Shindo, Y., Narita, F. and Ozawa, E., Impact response of a finite crack in an orthotropic piezoelectric ceramic., *Acta Mechanica 137*, 99-107, 1999.

(10) Sosa, Horacio and Khutoryansky, Naum, New developments concerning piezoelectric materials with defects. *Int. J. Solids Structures Vol. 33, No. 23.* pp. 3399-3414, 1996.